# Interaction of molecules with localized surface plasmons in metallic nanoparticles

T. J. Davis, D. E. Gómez, and K. C. Vernon
*CSIRO Materials Science and Engineering, Private Bag 33, Clayton, Victoria 3168, Australia*
*and CSIRO Future Manufacturing Flagship, Gate 5 Normanby Road, Clayton, Victoria 3168, Australia*
(Received 19 October 2009; revised manuscript received 15 December 2009; published 29 January 2010)

A theory is developed to model the interaction of molecules with the localized surface plasmon resonances in metallic nanoparticles that are used for single-molecule sensing. Each molecule is represented by a simple point-like dipole based on a dielectric sphere, taken in the limit of a small radius. The surface-charge and surface-dipole eigenfunctions of a small spherical particle are represented analytically and it is shown that these are natural extensions of the electrostatic coupling theory of Davis *et al.* [Phys. Rev. B **79**, 155423 (2009)]. The effect of a molecule on the surface plasmon resonances is described in terms of an effective background permittivity and formulas for the frequency and phase shifts of the resonances are obtained that depend on the polarizability of the molecule, the eigenvalues associated with the nanoparticle resonances and the strength of the geometric coupling. The interaction of the point-like dipoles with surface charges of different distributions is studied and it is shown that for molecules that cannot approach closer to the nanoparticle than a fixed distance, there is an optimum dimension of the nanoparticle to obtain the maximum coupling. This is important for the optimum design of nanoparticle-based sensors. Analytical expressions for the coupling of molecules to nanoparticles are obtained for some simple geometries and the results are compared with numerical simulations.

DOI: 10.1103/PhysRevB.81.045432 PACS number(s): 78.67.Bf, 73.20.Mf, 78.20.Bh, 87.85.fk

## I. INTRODUCTION

Localized surface plasmon resonances in metallic nanoparticles provide sensitive measures of changes to the electric permittivity of the local environment. The surface plasmon resonances are easily observed in the spectrum of light scattered from the nanoparticle and their resonance frequencies change with the surrounding electric permittivity.[1–6] In particular, the presence of molecules in solution near to the nanoparticle also alters the electric permittivity and can be detected by these spectral shifts, providing a means for sensing the changes to the local chemical environment. This has generated substantial interest in the use of metallic nanoparticles for sensing[7–12] with the ultimate goal to detect the presence of individual molecules.[11,12] Most of these works have concentrated on the effects of the surrounding bulk dielectric on the changes in the resonances for a range of nanoparticle geometries such as ellipsoids and tetrahedrons,[1] spheres,[2,4] disks,[3,6] triangles,[4,7] cylinders,[6] and spherical shells.[5,6,8] The effect of the substrate on the localized surface plasmon resonances has also been investigated for lithographically patterned nanoparticles[13] and for spherical plasmonic nanoparticles.[14]

For single-molecule sensing it is important to understand the effects of a small number of molecules, particularly for nanostructures with geometries that can support more complex resonant modes. The effects of molecules on coupled systems are also important, where the change in the permittivity around one nanostructure will influence the resonances of a nearby nanostructure.[15] This is due to coupling between the electric near fields of the nanoparticles which has the potential to affect the response of the entire system. In this regard it is useful to know where the system is most sensitive to the presence of a molecule. For example, we would expect low sensitivity if the molecules bind to portions of the nanoparticle where the electric fields are small.

In this paper we model the effect of a molecule on the localized surface plasmon resonances associated with one or more metallic nanoparticles. A simple method for modeling the interactions in an ensemble was described recently[16] in terms of the electric coupling between nanoparticles. The coupling theory is based on an electrostatic approximation[17] in which the nanoparticles are assumed to be much smaller than the wavelength of the incident light. In this size regime the electric and magnetic fields decouple and the nanoparticles appear to be in a spatially uniform but time varying electric field. In this paper we further develop the theory to include the effects of a molecule on the resonances of a single nanoparticle or an ensemble. By treating each molecule as a point-like dipole, modeled by a dielectric sphere in the small radius limit, we derive the dipole eigenfunctions that allow it to be included in the electrostatic coupling theory in a natural manner. Our specific intention is to determine the effect of the molecule and its proximity to the nanostructure on the surface plasmon resonances with particular focus on the shifts in the resonant frequency and the phase. Moreover, we would like to determine the optimum conditions to couple a molecule to a nanostructure so that we can maximize the change in the surface plasmon resonance.

Although the interaction of single molecules with metallic nanostructures has not been well studied from the point of view of sensing, the interaction of an oscillating dipole with metallic surfaces has received considerable attention in relation to fluorescence and surface-enhanced Raman scattering.[18–25] In effect, the dipole interacts with its image charge in the metal leading to enhancement or suppression of the emission depending on the distance between the dipole and the surface. Similar damping effects are observed with dipoles in metallic cavities.[26]

The electromagnetic interactions between a molecule and a metal surface were reviewed by Ford and Weber[27] who discuss the electrostatic approximation and compare local

 

with nonlocal theories of the electric permittivity. There are two key points that should be noted from this review that relate to our use of the electrostatic approximation. This approximation is valid in the limit where the dimensions of the system of nanostructures are smaller than the wavelength of the radiation in the surrounding medium. The second point is that we assume in the electrostatic theory that the permittivity of the metal is adequately described by a local interaction. That is, the permittivity does not depend on the wavelength of the resonances in the metallic nanostructure. This is satisfied provided that the structures are significantly larger than the Fermi wavelength of the electrons in the metal. For gold or silver, which are used typically for plasmonic nanoparticles, this requires dimensions greater than about $1/k_F \approx 0.1$ nm for a Fermi wavenumber $k_F$. This also means that our analysis will be in error for distances closer than about 0.1 nm to the metal surface.

In Sec. II we briefly review the theory of the coupling of localized surface plasmons in nanoparticles based on the electrostatic approximation. The advantage of the theory is that it enables us to derive analytical expressions that are independent of the shape of the nanoparticle. We further develop the theory by representing a molecule by a point-like dipole, obtained from the properties of a dielectric sphere in the limit where the radius becomes very small. Analytical forms for the surface-charge and surface-dipole eigenfunctions of the sphere are deduced which enables us to represent the molecule in terms of the parameters of the coupling theory.

In Sec. III, we consider the interaction of a molecule with the resonant modes of a nanoparticle. By taking only one resonance as dominant and neglecting image charges, we derive an expression for the shift in the amplitude of the resonance of the nanoparticle due to the presence of the molecule. This enables us to derive formulas relating the change in the electric permittivity, the shift in the resonance and the shift in the phase in terms of the dielectric properties of the molecule and its proximity to the nanoparticle.

Then in Sec. IV we consider some simple situations where we can evaluate the coupling coefficients analytically. These expressions provide some useful properties of the interaction and indicate how we might optimize the influence of the molecule on the resonances.

The coupling formulas are applied to two simple situations in Sec. V where the molecule interacts with the hemispherical surface of a nanorod and with the center of a nanodisk. The distance dependence of the coupling is derived and compared with numerical results.

A summary and conclusions are given in Sec. VI.

## II. DIPOLES AND COUPLING THEORY

In this section we describe the interaction of a dipole with an ensemble of metallic nanoparticles using the electrostatic coupling theory.[16] We first review the main aspects of the theory and then investigate the interaction of a dielectric sphere with a uniform electric field. The problem is then recast in a form that allows the dipole model to become a natural part of the theory.

### A. Electrostatic coupling theory

In the electrostatic approximation, it is assumed that the metallic nanoparticles are much smaller than the wavelength of the incident light. Then the electromagnetic field surrounding a particle can be determined by solving for the self-sustained distribution of surface-charge $\sigma_q^k(\vec{\mathbf{r}})$ or surface-dipoles $\tau_q^k(\vec{\mathbf{r}})$ across the surface of the nanoparticle. These represent the eigenfunction solutions for the $k$-th mode of the $q$-th nanoparticle and are associated with eigenvalue $\gamma_q^k$. The eigenfunctions form a biorthogonal set that obeys the relationship

$$\oint \tau_p^j(\vec{\mathbf{r}})\sigma_q^k(\vec{\mathbf{r}})dS = \delta_{pq}\delta^{jk}, \tag{1}$$

which involves an integral over the surface $S$ of the nanoparticle. The resonant frequencies are determined by the eigenvalues and the frequency-dependent electric permittivity $\epsilon(\omega)$ of the nanoparticle, according to

$$\mathrm{Re}\ \epsilon(\omega_k) = \epsilon_b\left(\frac{1+\gamma_q^k}{1-\gamma_q^k}\right), \tag{2}$$

where $\omega_k$ is the resonant frequency associated with eigenvalue $\gamma_q^k$ and where $\epsilon_b$ is the permittivity of the background medium. The resonant frequency is found by selecting the background medium in which the nanoparticle is embedded and then finding the frequency that gives a metal permittivity that satisfies Eq. (2). An oscillating external electric field applied to a nanoparticle excites a surface-charge distribution $\sigma_q(\vec{\mathbf{r}},\omega)$ that can be represented by a superposition of the surface-charge eigenfunctions $\sigma_q^k(\vec{\mathbf{r}})$

$$\sigma_q(\vec{\mathbf{r}},\omega) = \sum_k a_q^k(\omega)\sigma_q^k(\vec{\mathbf{r}}). \tag{3}$$

The frequency-dependent coefficient $a_q^k(\omega)$ in the expansion is related to the strength of the applied field $\vec{\mathbf{E}}_0$ that excites the resonance and is given by[28]

$$a_q^k(\omega) = \frac{2\gamma_q^k\epsilon_b[\epsilon(\omega)-\epsilon_b]}{\epsilon_b(\gamma_q^k+1)+\epsilon(\omega)(\gamma_q^k-1)}\oint \tau_q^k(\vec{\mathbf{r}}_q)\hat{n}_q \cdot \vec{\mathbf{E}}_0 dS_q$$
$$= f_q^k\oint \tau_q^k(\vec{\mathbf{r}}_q)\hat{n}_q \cdot \vec{\mathbf{E}}_0 dS_q, \tag{4}$$

where $\hat{n}_q$ is the unit normal to the surface at $\vec{\mathbf{r}}_q$ and we have introduced the resonance factor $f_q^k$. The resonance condition Eq. (2) arises from Eq. (4) where the amplitude becomes large when the real part of the denominator goes to zero.

When there are multiple nanoparticles present, there are interactions between the electric fields arising from the localized surface plasmons and the surface-dipoles $\tau_q^k$ that modify the resonances. In the electrostatic coupling theory,[16] the presence of $N$ nanoparticles alters the single nanoparticle amplitudes $a_q^k$ in Eq. (4) according to

$$\tilde{a}_p^j(\omega) = \sum_{q=1}^{N} \sum_k [\delta_{pq}\delta^{jk} - C_{qp}^{kj}(\omega)]^{-1} a_q^k(\omega), \tag{5}$$

which is in the form of a matrix equation. The coupling coefficient $C_{pq}^{jk}(\omega)$ is given by

$$C_{pq}^{jk}(\omega) = \frac{f_p^j(\omega)}{4\pi\epsilon_b} \oint\oint \tau_p^j(\vec{\mathbf{r}}_p) \frac{\hat{n}_p \cdot (\vec{\mathbf{r}}_p - \vec{\mathbf{r}}_q)}{|\vec{\mathbf{r}}_p - \vec{\mathbf{r}}_q|^3} \sigma_q^k(\vec{\mathbf{r}}_q) dS_q dS_p, \tag{6}$$

and is defined so that $C_{qq}^{jk}=0$. The coupling represents the interaction of the electric field arising from surface-charge $\sigma_q^k(\vec{\mathbf{r}}_q)$ at $\vec{\mathbf{r}}_q$ with the surface-dipole $\tau_p^j(\vec{\mathbf{r}}_p)$ at $\vec{\mathbf{r}}_p$.

The eigenfunction approach to modeling the coupling has the advantage of relatively simple analytical expressions that are applicable to nanoparticles of any geometry. The coupling formula, Eq. (5), relates the coupling between all nanoparticles in the ensemble and all of their resonant modes. However, for many applications there is only one dominant resonance for each particle that is close to the frequency of the applied radiation field so that the coupling formula becomes quite simple. It is then possible to deduce many of the properties of the coupled system without needing to evaluate the coupling coefficient, Eq. (6). This is the advantage of this simple system based on the electrostatic approximation. Although the method is only approximate, particularly for larger nanoparticle systems, it provides a framework for designing structures with desired properties, such as the plasmonic "Wheatstone bridge."[15] Examples of this method applied to two and three particle systems are given in the literature.[16,29] It is of interest to note that the eigenfunction approach was previously used to develop a representation for the scattering spectrum from composite materials and grains.[30,31]

In the following section we will represent the effect of a set of molecules on the resonances of the nanoparticle ensemble using the coupling theory. This is done by modeling the response of a molecule by a point-like dipole and finding analytical expressions for the dipole eigenfunctions.

### B. Eigenfunctions for a dielectric sphere in a uniform electric field

A molecule can be modeled by a point-like dipole that responds to an applied electric field in the same way as a dielectric sphere, in the limit where the radius is very small. The polarization $\vec{\mathbf{P}}$ of a dielectric sphere in a uniform electric field $\vec{\mathbf{E}}$ is given by[32]

$$\vec{\mathbf{P}} = 3\epsilon_b \left( \frac{\epsilon_s - \epsilon_b}{2\epsilon_b + \epsilon_s} \right) \vec{\mathbf{E}} = f_s \vec{\mathbf{E}}, \tag{7}$$

where $f_s$ is the same resonance factor defined in Eq. (4) and where the eigenvalue for the dipole moment of the sphere is $\gamma_s=3$. The surface-charge density associated with the sphere is obtained from the boundary condition for the normal components of the polarization applied across the sphere surface. If we define $\hat{n}_s(\vec{\mathbf{r}}_s)$ as the surface normal at a point $\vec{\mathbf{r}}_s$ on the surface of the sphere, then the surface-charge density $\sigma_s(\vec{\mathbf{r}}_s, \omega)$ is

$$\sigma_s(\vec{\mathbf{r}}_s, \omega) = \hat{n}_s(\vec{\mathbf{r}}_s) \cdot \vec{\mathbf{P}} = f_s(\omega) \hat{n}_s(\vec{\mathbf{r}}_s) \cdot \vec{\mathbf{E}}. \tag{8}$$

Our aim is to write Eq. (8) in terms of a sum over surface-charge eigenfunctions, as in Eq. (3), with an amplitude given by the form of Eq. (4). Careful examination of Eq. (8) will show that it is almost in this form as it contains the resonance factor $f_s$ and a unit vector in the direction of the surface normal. The surface normal to the sphere can be written in spherical coordinates as $\hat{n}_s = \cos\theta\cos\phi\hat{x}_1 + \cos\theta\sin\phi\hat{x}_2 + \sin\theta\hat{x}_3$ in terms of the three unit vectors $\hat{x}_i$. If the electric field is aligned parallel to any one of the three component directions, Eq. (8) shows that the surface-charge distribution of the sphere has an angular dependence given by the corresponding component of the surface normal. In effect, each component of this vector defines a surface-charge distribution with a dipole moment oriented in one of three orthogonal directions. We can then identify three surface-charge eigenfunctions for the sphere, one for each component of the vector $\hat{n}_s$:

$$\sigma_s^1(\phi,\theta) = N_\sigma \cos\theta\cos\phi,$$

$$\sigma_s^2(\phi,\theta) = N_\sigma \cos\theta\sin\phi,$$

$$\sigma_s^3(\phi,\theta) = N_\sigma \sin\theta, \tag{9}$$

where $N_\sigma$ is a normalization factor that we will determine later. These functions, which are equivalent to the components of the spherical harmonics[27,32] of order $l=1$, allows us to rewrite Eq. (8) in the form of a sum over the unit vectors

$$f_s(\omega)\hat{n}_s(\vec{\mathbf{r}}_s) \cdot \vec{\mathbf{E}}_0 = \sum_{k=1}^{3} \sigma_s^k(\phi,\theta) f_s^k(\omega) \hat{x}_k \cdot \vec{\mathbf{E}}_0, \tag{10}$$

where the three eigenvalues $\gamma_s^k=3$ implicit in $f_s^k(\omega)$ have the same value, which means that the three surface-charge eigenfunctions are degenerate. Finally, we note the following relation between the product of each component of the unit vector $\hat{n}_s$ integrated over the surface of the sphere of radius $R_s$, $\oint(\hat{x}_k \cdot \hat{n}_s)\hat{n}_s dS = (4\pi R_s^2/3)\hat{x}_k$ which enables us to write

$$f_s^k(\omega)\hat{x}_k \cdot \vec{\mathbf{E}}_0 = (4\pi R_s^2/3)^{-1} f_s^k(\omega) \oint (\hat{x}_k \cdot \hat{n}_s)\hat{n}_s \cdot \vec{\mathbf{E}}_0 dS. \tag{11}$$

Comparing this with Eq. (4) identifies the surface-dipole eigenfunctions as

$$\tau_s^1(\phi,\theta) = N_\tau \cos\theta\cos\phi,$$

$$\tau_s^2(\phi,\theta) = N_\tau \cos\theta\sin\phi,$$

$$\tau_s^3(\phi,\theta) = N_\tau \sin\theta, \tag{12}$$

where $N_\tau$ is an appropriate normalization factor. These eigenfunctions are the same as for the surface-charge distributions.

The normalization factors can be found from the biorthogonal condition Eq. (1) which yields for a sphere of radius $R_s$

$$\oint \tau_s^j(\vec{\mathbf{r}})\sigma_s^k(\vec{\mathbf{r}})dS = \frac{4\pi R_s^2}{3} N_\sigma N_\tau \delta^{jk}, \tag{13}$$

which requires that $N_\sigma N_\tau = 3/4\pi R_s^2$. This yields one value for the normalization. The other value is obtained by ensuring that the average dipole moments calculated from both the surface-charge and the surface-dipole eigenfunctions are numerically the same. Specifically we have

$$\vec{\mathbf{p}}_s^j = \oint \sigma_s^j(\vec{\mathbf{r}})\vec{\mathbf{r}}dS = \hat{x}_j N_\sigma 4\pi R_s^3/3 = \oint \tau_s^j(\vec{\mathbf{r}})\hat{n}_s dS$$
$$= \hat{x}_j N_\tau 4\pi R_s^2/3. \tag{14}$$

Simultaneously satisfying the biorthogonality condition and the average dipole moment equation leads to the normalization factors $N_\sigma = \sqrt{3/(4\pi R_s^3)}$ and $N_\tau = \sqrt{3/(4\pi R_s)}$.

We can show that the normalization conditions lead to the correct form for the dipole moment of the sphere. Specifically, in terms of the eigenfunctions and expansion coefficients, we now have the dipole moment given by

$$\vec{\mathbf{p}} = \sum_k a_s^k \oint \sigma_s^k(\vec{\mathbf{r}})\vec{\mathbf{r}}dS = \sqrt{\frac{4\pi R_s^3}{3}} \sum_k a_s^k \hat{x}_k. \tag{15}$$

For an applied electric field $\vec{\mathbf{E}}_0$, the expansion coefficients are given by

$$a_s^k = f_s^k \oint \tau_s^k(\vec{\mathbf{r}})\hat{n}_s \cdot \vec{\mathbf{E}}_0 dS = f_s^k \sqrt{\frac{4\pi R_s^3}{3}} \hat{x}_k \cdot \vec{\mathbf{E}}_0. \tag{16}$$

Combining the two equations together, expanding out the resonance factor $f_s^k$ and including the eigenvalue $\gamma_s^k = 3$ leads to an expression for the dipole moment of the sphere

$$\vec{\mathbf{p}} = \sum_k \frac{2\gamma_s^k \epsilon_b(\epsilon_s - \epsilon_b)}{\epsilon_b(\gamma_s^k + 1) + \epsilon_s(\gamma_s^k - 1)} \frac{4\pi R_s^3}{3} \hat{x}_k(\hat{x}_k \cdot \vec{\mathbf{E}}_0)$$
$$= \epsilon_b \left( 4\pi R_s^3 \frac{(\epsilon_s - \epsilon_b)}{2\epsilon_b + \epsilon_s} \right) \vec{\mathbf{E}}_0 = \epsilon_b \alpha \vec{\mathbf{E}}_0, \tag{17}$$

where the term in brackets on the last line has been replaced by $\alpha$, the polarizability.[33]

### C. Dipole coupling coefficients

The effect of a point-like dipole on an ensemble of nanoparticles can be easily included in the existing coupling theory using the coupling coefficient Eq. (6) together with the eigenfunctions Eqs. (9) and (12). This coupling coefficient can be evaluated analytically if we assume that the dimensions of the dipole are small compared to the distances between the dipole and neighboring particles. For the case where the electric field arising from the surface charge of the molecule couples to a neighboring nanoparticle, the vector difference $\vec{\mathbf{r}}_p - \vec{\mathbf{r}}_q$ is modified to $\vec{\mathbf{r}}_p - \vec{\mathbf{r}}_d - \vec{\delta}_d$ where $\vec{\mathbf{r}}_d$ points to the center of the dipole sphere and $\vec{\delta}_d$ is a vector from the center of the sphere to the surface. Since this vector is assumed to be small, the denominator in Eq. (6) can be approximated by $|\vec{\mathbf{r}}_p - \vec{\mathbf{r}}_d - \vec{\delta}_d|^{-3} \approx |\vec{\mathbf{r}}_p - \vec{\mathbf{r}}_d|^{-3}(1 + 3\vec{\delta}_d \cdot (\vec{\mathbf{r}}_p - \vec{\mathbf{r}}_d)/|\vec{\mathbf{r}}_p - \vec{\mathbf{r}}_d|^2)$ and the integration can be performed analytically. This results in the following expression for the coupling of a point-like dipole with a surface-dipole distribution

$$C_{pd}^{jk}(\omega) \approx \frac{f_p^j(\omega)}{4\pi\epsilon_b} \sqrt{\frac{4\pi R_d^3}{3}}$$
$$\times \oint \tau_p^j(\vec{\mathbf{r}}_p) \frac{\hat{n}_p \cdot (3\hat{n}_{pd}(\hat{n}_{pd} \cdot \hat{x}_k) - \hat{x}_k)}{|\vec{\mathbf{r}}_p - \vec{\mathbf{r}}_d|^3} dS_p, \tag{18}$$

where $\hat{n}_{pd}$ is the unit vector from the dipole $d$ to particle $p$. Equation (18) contains the well-known form of the electric field from a point-like dipole[32] at $\vec{\mathbf{r}}_d$ interacting with a surface dipole at $\vec{\mathbf{r}}_p$. Applying the same approximation to the interaction of a surface-charge distribution to a point-like dipole at $\vec{\mathbf{r}}_d$ yields for the coupling coefficient

$$C_{dp}^{jk}(\omega) \approx \frac{f_d^j(\omega)}{4\pi\epsilon_b} \sqrt{\frac{4\pi R_d^3}{3}} \oint \frac{\hat{x}_j \cdot (\vec{\mathbf{r}}_d - \vec{\mathbf{r}}_p)}{|\vec{\mathbf{r}}_d - \vec{\mathbf{r}}_p|^3} \sigma_p^k(\vec{\mathbf{r}}_p) dS_p, \tag{19}$$

which represents the coupling of the electric field from a surface-charge distribution to a dipole oriented in direction $\hat{x}_j$. In these equations $R_d$ is the effective radius of the molecule which equals the radius of the sphere used in the model.

## III. COUPLING OF A MOLECULE TO A RESONANT METALLIC NANOPARTICLE

The coupling coefficients are important for determining the effect of a molecule on the resonances of a nanoparticle. In this section we derive a relation between the shift in the resonance and the properties of the molecule as modeled by an equivalent dipole. The end result is an expression for the effective permittivity surrounding the nanoparticle that is responsible for a shift in the frequency of the localized surface plasmon resonances. Although we only consider the case where the dipole is not resonant, it still may couple to many of the high-order eigenmodes of the nanoparticle.

The effect of the electric coupling between the dipole and the nanoparticle is obtained from Eq. (5). We first consider the matrix $(\delta_{pd}\delta^{jk} - C_{pd}^{jk})$ associated with a single nanoparticle, labeled by $p$ with $N$ modes, coupled to a single dipole $d$. In our simple analyses of Sec. IV, we will find that the coupling to the dipole is predominantly to one of its modes. In this section, for simplicity, we assume that the dipole is oriented such that the coupling of the nanoparticle is to a single mode $k$ representing the orientiation $\hat{x}_k$ of the dipole. Furthermore, we note that the modes of the nanoparticle do not couple to one another. In this case the matrix takes the form

$$\begin{pmatrix} 1 & 0 & \cdots & 0 & -C_{pd}^{1k} \\ 0 & 1 & \cdots & 0 & -C_{pd}^{2k} \\ \cdots & \cdots & \cdots & \cdots & \cdots \\ 0 & 0 & \cdots & 1 & -C_{pd}^{Nk} \\ -C_{dp}^{k1} & -C_{dp}^{k2} & \cdots & -C_{dp}^{kN} & 1 \end{pmatrix}. \tag{20}$$

The inverse of this matrix, as required in Eq. (5), involves the determinant $\Delta$ given by

$$\Delta = 1 - \sum_{n=1}^{N} C_{dp}^{kn} C_{pd}^{nk}, \tag{21}$$

that depends on combinations of coupling coefficients between the dipole and the nanoparticle eigenfunctions. The mode of interest is the resonant low-order mode that is likely to dominate the sum. We remove this term from the sum to show it explicitly and then represent the effects of all the nonresonant modes of the nanoparticle by a separate term. Labeling the resonant mode by $j=1$ then

$$\sum_{n=1}^{N} C_{dp}^{kn} C_{pd}^{nk} = C_{dp}^{k1} C_{pd}^{1k} + C_{dI} C_{Id}, \tag{22}$$

where $C_{dI}C_{Id}$ represents the coupling term associated with the nonresonant modes.

While it is tempting just to ignore these modes, they are necessary to account for the interaction of the dipole with its image charge. When the dipole is close to the metal, the dipole field interacts with the electrons in a small region on the surface. The perturbation of these electrons from their equilibrium constitutes the image charge of the dipole. The perturbation can be represented by a large number of high-order eigenmodes of the nanoparticle. These modes are associated with high spatial frequencies and are necessary to represent the local charge distribution. Although the interaction of the dipole with each mode may be small, the sum of all of these interactions is a representation of the coupling of the dipole with its image charge. We estimate the magnitude of this term by assuming a plane surface for the nanoparticle. This is appropriate in the limit where the dipole is very close to the nanoparticle surface.[27] Then the image-charge coupling has the form

$$C_{dI}C_{Id} \approx \frac{\alpha}{8\pi^2}\left(\frac{\epsilon - \epsilon_b}{\epsilon + \epsilon_b}\right)\frac{3(\hat{n}_{di} \,.\, \hat{x}_k)^2 - 1}{|\vec{r}_d - \vec{r}_i|^3}, \tag{23}$$

where the dipole is located at $\vec{r}_d$, its image is at $\vec{r}_i$ and the unit vector from the image to the dipole is $\hat{n}_{di}$. The definition of the polarizability $\alpha$ in Eq. (17) contains a factor $R_d^3$. Since the distance between the dipole and its image must be at least twice the dipole radius, so that $|\vec{r}_d - \vec{r}_i|^3 > 8R_d^3$, then the image-charge coupling is such that $C_{dI}C_{Id} \ll 1$. These terms always appear in the form $1 - C_{dI}C_{Id}$ so that, for the purposes of determining the shifts of the resonances, we will ignore the image-charge coupling term. This may not be valid if either the dipole is resonant, so that $2\epsilon_b + \epsilon_d = 0$ and $\alpha$ becomes large, or the nanoparticle exhibits a high-order resonance where $\mathrm{Re}(\epsilon + \epsilon_b) = 0$. In both cases the image charge may be large. In the following we assume that these terms are always small.

Let $a_p^1$ be the excitation amplitude associated with mode $j=1$ of an isolated nanoparticle. Then the excitation amplitude $\tilde{a}_p^1$ of the particle in the presence of mode $k$ of a dipole $d$ is given by

$$\tilde{a}_p^1 = \frac{(\Delta + C_{pd}^{1k} C_{dp}^{k1}) a_p^1 + C_{pd}^{1k} a_d^k + \sum_{n=2}^{N} C_{pd}^{1k} C_{dp}^{kn} a_p^n}{\Delta}, \tag{24}$$

where $a_d^k$ is the excitation amplitude of the dipole. This is a solution of Eq. (5) using the matrix Eq. (20). The last term in Eq. (24) is the contribution to the amplitude $\tilde{a}_p^1$ of the higher-order eigenmodes excited by the incident light. These couple to the resonant mode by interaction with the dipole. Taking these terms and the image-charge coupling terms as small, then

$$\tilde{a}_p^1 \approx \frac{a_p^1 + C_{pd}^{1k} a_d^k}{1 - C_{dp}^{k1} C_{pd}^{1k}}. \tag{25}$$

The excitation amplitude of the dipole can be replaced by Eq. (16) in terms of the direction $\hat{x}_k$ of mode $k$. Similarly, $a_p^1$ can be replaced by an expression for the dipole moment $\vec{\mathbf{p}}_p^1$ associated with the surface-charge eigenfunction $\sigma_p^1$ such as in Eq. (14).

It is also convenient to separate out the resonance factors $f_p^j$ from the coupling coefficients by defining terms $\eta_{pd}$ that contain only the geometry

$$C_{pd}^{jk} = \frac{f_p^j}{4\pi\epsilon_b}\sqrt{\frac{4\pi R_d^3}{3}}\,\eta_{pd}, \tag{26}$$

which allows us to write

$$\tilde{a}_p^1 = \frac{f_p^1(\vec{\mathbf{p}}_p^1 + (\eta_{pd}/4\pi)\alpha\hat{x}_k) \,.\, \vec{\mathbf{E}}_0}{1 - (f_p^1/16\pi^2\epsilon_b)\alpha\eta_{pd}\eta_{dp}}, \tag{27}$$

where the resonance factor of the dipole has been replaced by its polarizability $\alpha$, as in Eq. (17). The resonance of the nanoparticle occurs at the frequency where the denominator in Eq. (27) is zero. This involves the resonance factor $f_p^1$ of the nanoparticle. Equating the denominator to zero and expanding out the resonance factor yields

$$\epsilon(\omega) = \epsilon_{\mathrm{eff}}\left(\frac{1 + \gamma_p^1}{1 - \gamma_p^1}\right), \tag{28}$$

where the effective background electric permittivity is defined by

$$\epsilon_{\mathrm{eff}} = \epsilon_b\left\{\frac{1 + (\gamma_p^1\alpha\eta_{pd}\eta_{dp})/[8\pi^2(1+\gamma_p^1)]}{1 + (\gamma_p^1\alpha\eta_{pd}\eta_{dp})/[8\pi^2(1-\gamma_p^1)]}\right\}. \tag{29}$$

This describes the influence of a molecule on the localized surface plasmon resonance in terms of an effective shift in the permittivity of the surrounding medium. The effective permittivity depends on the polarizability of the molecule and also on the resonant mode of the nanoparticle through the eigenvalue $\gamma_p^1$. The largest resonance shifts are obtained by maximizing the geometric coupling and minimizing the eigenvalue. With localized surface plasmon resonances, the eigenvalue $\gamma_p^1 > 1$ and it becomes close to unity when the nanoparticle is much longer than it is wide. This suggests that for applications requiring high sensitivity the nanoparticles should have a high aspect ratio such as a long rod.

For the coupling of small numbers of molecules to the nanoparticle, the coupling terms and the polarizability are small so that the effective permittivity can be approximated by

$$\epsilon_{\text{eff}} \approx \epsilon_b \left( 1 + \frac{\alpha \gamma_p^{1^2} \eta_{pd} \eta_{dp}}{4\pi^2 (\gamma_p^{1^2} - 1)} \right). \tag{30}$$

Alternatively we can write an expression for the change in the metal electric permittivity required for the nanoparticle to resonate

$$\frac{\epsilon(\omega) - \epsilon(\omega_0)}{\epsilon(\omega_0)} \approx \frac{\alpha \gamma_p^{1^2} \eta_{pd} \eta_{dp}}{4\pi^2 (\gamma_p^{1^2} - 1)}, \tag{31}$$

where $\epsilon(\omega_0)$ is the metal permittivity that gives rise to the resonance at frequency $\omega_0$ in the absence of the molecules, as would be evaluated using Eq. (2). Once the functional form of the metal permittivity is known, the shift $\delta\omega$ in the resonant frequency can be evaluated. For example, the shift in the resonance of a nanoparticle with a permittivity described by the Drude model is given by

$$\delta\omega \approx -\omega_0 \left( \frac{\omega_p^2 - \omega_0^2}{2\omega_p^2} \right) \frac{\alpha \gamma_p^{1^2} \eta_{pd} \eta_{dp}}{4\pi^2 (\gamma_p^{1^2} - 1)}, \tag{32}$$

where $\omega_p$ is the plasma frequency. The shift is toward lower frequencies or longer wavelengths of the scattered light.

For a real metal which involves losses, there is an imaginary term in the expression for the electric permittivity. The nanoparticle will resonate $\pi/2$ out of phase with the applied light field when it is driven at its resonant frequency. However, the presence of a molecule will shift the resonant frequency according to Eq. (32) which will cause a shift in the phase of the nanoparticle resonance. This phase shift is proportional to the polarizability of the molecule and it can be measured using plasmonic systems such as the plasmonic Wheatstone bridge.[15] If the imaginary part of the permittivity is written as Im $\epsilon$, then for small phase shifts $\Delta\phi$ away from resonance we find that

$$\Delta\phi \approx -\left( \frac{\alpha \gamma_p^{1^2} \eta_{pd} \eta_{dp}}{4\pi^2 (\gamma_p^1 - 1)^2} \right) \left( \frac{\epsilon_b}{\text{Im } \epsilon} \right). \tag{33}$$

This equation derives from Eq. (27) by resolving the denominator into real and imaginary components and taking their ratio. In the approximation we have assumed that the imaginary component of the permittivity is small compared to $2\gamma_p^1 \epsilon_b / (\gamma_p^1 - 1)$. The phase shift in the resonance of the nanoparticle is proportional to the polarizability of the molecule and depends on the strength of the coupling. Estimates of the effect of a molecule near a resonant nanoparticle are given in the following section, based on simple formulas for the coupling coefficients and numerical simulations.

## IV. COUPLING TO SIMPLE NANOPARTICLE GEOMETRIES

We now consider the interaction of a point-like dipole with distributions of surface dipoles and surface charges, through the coupling formulas Eqs. (18) and (19). We will develop analytical formulas for some simple geometries that approximate actual nanoparticles. This will provide some insight into the nature of the coupling and its dependencies on the nanoparticle geometry. One of the types of structures we will consider later are gold nanorods[34] such as those shown in Fig. 1. These consist of cylinders with ends that are approximately hemispherical. Note that, although the expressions for the coupling coefficients depend on $|\vec{\mathbf{r}}_p - \vec{\mathbf{r}}_d|^{-3}$, the surface charges and surface dipoles are not located at a point but are surface distributions. This has the effect of removing the infinity at $\vec{r}_p = \vec{r}_d$ when the point-like dipole rests on the surface of the nanoparticle.

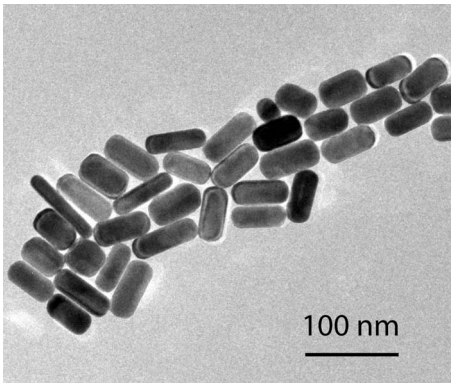


FIG. 1. A TEM image of an ensemble of gold nanorods created using chemical synthesis. The rods are cylindrical in shape with ends that are approximately hemispheres.

In the following sections we consider a number of cases involving the point-like dipole and distributions of surface charges, surface dipoles, and curved surfaces. We will use a coordinate system $\hat{x}$, $\hat{y}$, and $\hat{z}$ that will also be represented by $\hat{x}_i$ and we shall use these symbols interchangeably.

### A. Constant surface distribution over a disk

Consider a constant surface-dipole distribution $\tau_p^0$ over the $x$-$y$ plane with a surface normal $\hat{n}_p = \hat{x}_3$. We place the dipole at a height $z_d$ above the origin, so that $\vec{\mathbf{r}}_d = z_d \hat{x}_3$. A vector to a point in the plane is $\vec{\mathbf{r}}_p = r(\cos\phi \hat{x}_1 + \sin\phi \hat{x}_2)$ so that the difference is $|\vec{\mathbf{r}}_p - \vec{\mathbf{r}}_d|^2 = r^2 + z_d^2$. Evaluating Eq. (18) radially out to a distance $R_p$ on the plane gives for the coupling coefficient

$$C_{pd}^{0k} = \frac{f_p^0 \tau_p^0 (\hat{x}_k \cdot \hat{x}_3)}{4\pi\epsilon_b} \sqrt{\frac{4\pi R_d^3}{3}} \frac{2\pi R_p^2}{(R_p^2 + z_d^2)^{3/2}}. \tag{34}$$

Immediately we see that only the component of the dipole field parallel to the surface normal will couple to the surface-dipole distribution. The coupling coefficient is maximum when the dipole is resting on the surface, so that $z_d = 0$. However, in practise the molecules, represented by the point-like dipoles, will have a finite size. For example, complex organic molecules such as proteins may be quite large so that, when modeled as spheres, their centers may be several nanometers from the surface, $z_d \geq R_d$. In this case we may consider $z_d$ as a fixed quantity and maximize the coupling with respect to

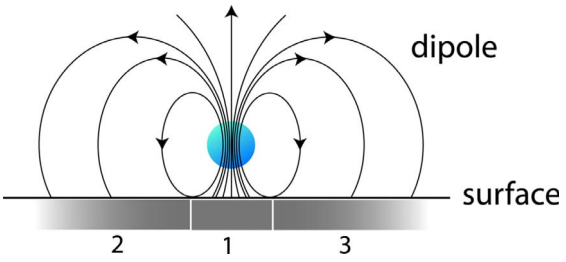


FIG. 2. (Color online) The interaction of a dipole with a surface showing the reversal of the field from beneath the dipole in region 1 to the regions 2 and 3 that reduce the coupling.

the dimension of the surface-dipole distribution. From Eq. (34) we note that the coupling is zero for $R_p=0$ but it also approaches zero as $R_p\to\infty$. The maximum coupling occurs for $R_p=\sqrt{2}z_d$. The reason for this is related to the electric field distribution surrounding the dipole (Fig. 2). For the dipole aligned parallel with the surface normal, the electric field immediately below it is parallel to the surface-dipoles. In this case it contributes significantly to the coupling. However, at some distance from the dipole, the electric field reverses direction so that it is antiparallel to the surface-dipole distribution. As the radius $R_p$ of the surface-dipole region increases, there is a greater contribution of the antiparallel field to the coupling coefficient, which subtracts from the parallel contribution and reduces the overall coupling. The point where the field from the dipole is perpendicular to the surface normal occurs at a distance $R_p=\sqrt{2}z_d$ and so the coupling is maximum over this distance.

The reverse coupling, namely that of a surface-charge distribution to the point-like dipole, is obtained from Eq. (19). The integration is straightforward, leading to the result

$$C_{dp}^{k0}=\frac{f_d^k\sigma_p^0(\hat{x}_k\,.\,\hat{x}_3)}{4\pi\epsilon_b}\sqrt{\frac{4\pi R_d^3}{3}}2\pi\left(1-\frac{z_d}{\sqrt{R_p^2+z_d^2}}\right). \quad (35)$$

When the dipole is placed on the surface, we have a finite value for the coupling which is equivalent to the electric field arising from an infinite surface of charge. The same result is obtained for large radius $R_p\to\infty$ where the coupling becomes independent of height above the surface. For a surface charge of a finite size, the coupling falls to zero as the dipole moves away from the surface, as we would expect.

### B. Hemispherical surface distribution

In this section we consider a uniform surface-dipole distribution $\tau_p^k$ over the surface of a hemisphere of radius $R_p$. Hemispheres provide useful models of the ends of a nanoparticle rod that supports a resonant dipole mode. For a conducting sphere in a uniform electric field, the surface charge distribution has a cos $\theta$ dependence on angle[32] so that the surface charge is approximately uniform in the region of the sphere where $\theta\approx 0$, which would correspond to the region about the end of the nanorod. From our electrostatic calculations we usually find that the surface-charge and surface-dipole distributions over the hemisphere are relatively uniform suggesting that the cylindrical body of the rod reduces the dependence on $\theta$. To keep the calculations simple, we approximate the surface-charge and surface-dipole distributions as constants over the hemisphere. In our model we place the dipole above the center of the hemisphere at a distance $z_d$ from the top. With the hemisphere centered on the origin, this gives $\vec{\mathbf{r}}_d=(R_p+z_d)\hat{x}_3$ and the vector to a point on the hemisphere is $\vec{\mathbf{r}}_p=R_p(\cos\theta\cos\phi\hat{x}_1+\cos\theta\sin\phi\hat{x}_2+\sin\theta x_3)$ where we are using a spherical coordinate system. With these definitions, the unit vectors $\hat{n}_p$ and $\hat{n}_{pd}$ can be determined and the integrals in Eq. (18) evaluated. The result is

$$C_{pd}^{0k}=\frac{f_p^0\tau_p^0(\hat{x}_k\,.\,\hat{x}_3)}{4\pi\epsilon_b}\sqrt{\frac{4\pi R_d^3}{3}}\frac{2\pi R_p^2}{(R_p^2+(R_p+z_d)^2)^{3/2}}, \quad (36)$$

which is the same as for the constant surface-dipole distribution over a disk of radius $R_p$. For a dipole at a fixed height $z_s$ above the hemisphere, the maximum coupling is obtained for a hemisphere radius of $R_p=z_d(\sqrt{17}+1)/4$. The coupling falls to zero for $R_p=0$, and for a very large radius, as $R_p\to\infty$.

The reverse coupling of a point-like dipole with a uniform surface-charge distributed over a hemisphere is given by

$$C_{dp}^{k0}=\frac{f_d^k\sigma_p^0(\hat{x}_k\,.\,\hat{x}_3)}{4\pi\epsilon_b}\sqrt{\frac{4\pi R_d^3}{3}}\times\frac{2\pi R_p^2}{(R_p+z_d)^2}\left(1+\frac{R_p}{\sqrt{R_p^2+(R_p+z_d)^2}}\right), \quad (37)$$

which is valid for $z_d\geq 0$. As the dipole moves away from the hemisphere, the coupling formula approaches that of an electric field from a point charge $Q=2\pi R_p^2\sigma_p^0$. Note that, as for the coupling of a point-like dipole with the surface, the coupling coefficient is zero for zero radius. However, in contrast with the coupling of a point-like dipole, it approaches a finite value as the radius becomes very large. This highlights the difference between the field from a surface-charge distribution and that from a dipole which are quite different in character.

### C. Linearly varying surface distribution

As a final example of coupling coefficients associated with surface-charge distributions, we now consider a linear variation over the $x$-$y$ plane. To begin with we determine the coupling coefficient for a surface-dipole distribution that varies linearly with distance. We choose the variation along the vector $\vec{\mathbf{r}}=r\cos\theta\hat{x}_1+r\sin\theta\hat{x}_2$ which represents a line at angle $\theta$ to the $x_1$ axis. The surface-dipole distribution then varies as $\tau_p^1 r\cos(\phi-\theta)$ where $\phi$ is the polar angle in the $x$-$y$ plane and $\tau_p^1$ is a constant. The surface normal is $\hat{n}_p=\hat{x}_3$ as before. The coupling of the point-like dipole with the surface-dipole distribution is

$$C_{pd}^{0k}=\frac{f_p^0\tau_p^1}{4\pi\epsilon_b}\sqrt{\frac{4\pi R_d^3}{3}}[\cos\theta(\hat{x}_k\,.\,\hat{x}_1)+\sin\theta(\hat{x}_k\,.\,\hat{x}_2)]\times 2\pi\left[\frac{z_d}{2}\frac{(3R_p^2+2z_d^2)}{(R_p^2+z_d^2)^{3/2}}-1\right]. \quad (38)$$

The linear variation is different from the constant surface

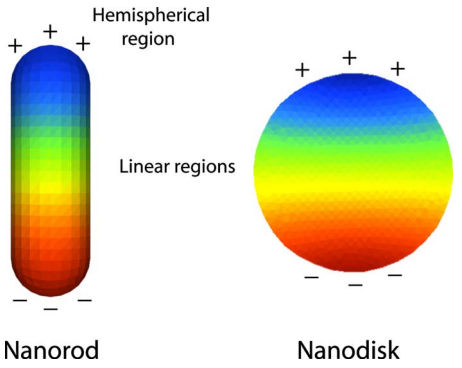


FIG. 3. (Color online) The surface-dipole distribution of the fundamental surface plasmon modes of a metallic nanorod and a metallic nanodisk. The color (gray level) represents the relative strength of the surface dipoles.

distribution in that the interaction with the normal-directed dipole is zero and the maximum field interaction is with the dipole aligned parallel to the surface variation. Note that we have limited the variation to a disk of radius $R_p$. The reverse coupling that of a surface-charge to the dipole is given by

$$C_{dp}^{k0} = \frac{f_d^k \sigma_p^1}{4\pi\epsilon_b}\sqrt{\frac{4\pi R_d^3}{3}}[\cos\ \theta(\hat{x}_k \cdot \hat{x}_1) + \sin\ \theta(\hat{x}_k \cdot \hat{x}_2)] \times 2\pi z_d\left(1 - \frac{1}{2z_d}\frac{R_p^2 + 2z_d^2}{\sqrt{R_p^2 + z_d^2}}\right). \quad (39)$$

## V. EFFECT OF MOLECULES ON SURFACE PLASMON RESONANCES

In this section we investigate the effect of molecules on the localized surface plasmon resonances of two different nanoparticles. The distance dependence of the coupling is determined using both the simple analytical formulas derived in the previous section and numerical calculations based on the coupling theory.[16] We consider the coupling to the fundamental dipole resonances of a nanorod and a nanodisk with surface-dipole distributions as shown in Fig. 3. For the nanorod, the distribution is relatively uniform around the surface of the hemispherical endcap so we would expect reasonable agreement between the analytical expressions and a numerical evaluation for the coupling of a molecule to this region. The surface of the nanodisk and the sides of the nanorod show approximately linear variations of the surface-dipole distributions. In this case we would expect a reasonable representation of the disk using our analytical formula for a linear surface-charge variation.

The numerical simulations are performed by representing the molecule by a small sphere. The eigenfunctions of the sphere are obtained by tesselating the surface with 600 triangles and using the numerical eigenvalue method discussed by Mayergoyz *et al.*[17] The fundamental resonance of the sphere is threefold degenerate and all three modes are used in the coupling theory[16] to deduce the geometry-dependent coupling terms $\eta_{pd}\eta_{dp}$ as functions of distance from the nanoparticle.

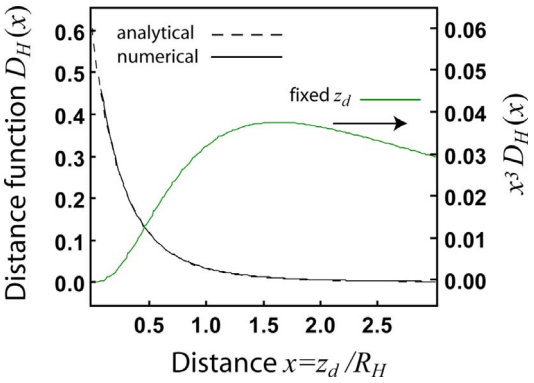


FIG. 4. (Color online) The distance dependent function $D_H(x)$ for coupling of a molecule to a hemisphere as a function of $x = z_d/R_H$. The dashed line is based on the analytical calculation whereas the solid black line is derived from a numerical simulation. Also included on the graph is the function $x^3 D_H(x)$ which indicates the variation of the coupling with the size of the coupling region for a fixed dipole distance $z_d$. This shows a maximum indicating an optimum size for coupling.

### A. Coupling to the nanorod

To evaluate the dependence of the effective permittivity on the geometry of the coupling, we first consider a dipole near the surface of the hemispherical cap on a nanorod. The factor $\eta_{pd}\eta_{dp}/8\pi^2$ in Eq. (29) contains the product of two eigenfunctions $\tau_p^0\sigma_p^0$ which, for a hemisphere, have been taken as constant. From Eq. (1) this product integrated over the surface of the nanoparticle must give unity. If we take the hemisphere to have radius $R_H$ and assume that the hemisphere represents a fraction $f_H$ of the total surface, then we can estimate $\tau_p^0\sigma_p^0 2\pi R_H^2 \approx f_H$ so that

$$\frac{\alpha\eta_{pd}\eta_{dp}}{8\pi^2} = (\hat{x}_k \cdot \hat{z})^2 f_H D_H(x)\left(\frac{R_d}{R_H}\right)^3\left(\frac{\epsilon_d/\epsilon_b - 1}{\epsilon_d/\epsilon_b + 2}\right), \quad (40)$$

where $x = z_d/R_H$ and the distance dependent term is

$$D_H(x) = \frac{1}{(x+1)^2(1+(x+1)^2)^{3/2}} \times \left(1 + \frac{1}{\sqrt{1+(x+1)^2}}\right). \quad (41)$$

Note that these functions are scale independent, consisting of ratios of distances and ratios of permittivities.

The distance function $D_H(x)$ is shown as the dashed line in Fig. 4. For small $z_d$ the function asymptotes to $(1+1/\sqrt{2})/2^{3/2} \approx 0.6$. However, as the radius of the hemisphere becomes large the coupling is dominated by the $(R_d/R_H)^3$ term so that large nanoparticles will have small resonance shifts associated with the presence of a molecule. The optimum situation is when the dipole is resting on the surface, so that $z_d = R_d$ and the radius of the hemisphere is small. This implies that the best coupling occurs for features that have a high radius of curvature. For such small features it is unlikely that the current theory would be adequate to describe the interactions, as discussed in the introduction.

However, for the sensing of large molecules, such as proteins, where the nanoparticle is combined with a chemical-selective coating, such as an antibody, the molecule will never come in contact with the surface. Rather, it will bind to the coating molecules at some fixed distance $z_d$ above the surface. In this situation, we find that there is an optimum hemisphere radius which arises from a trade off between the $R_H^{-3}$ term which favors a small radius and the function $D_H(z_d/R_H)$ that favors a large radius. The optimum hemisphere radius is obtained from $x^3D_H(x)$ as shown in Fig. 4 and it occurs for $x=1.625$ or $R_H \approx 0.62 z_d$.

To compare the analytical formula for the distance function with a numerical calculation, the nanorod is represented by a cylinder with hemispherical endcaps, as shown in Fig. 3. The surface is tesselated with 3520 triangles and the eigenfunctions found using the electrostatic method.[17] The coefficients for the coupling of the sphere to the fundamental mode of the nanorod are evaluated as a function of the distance of the sphere above the top of the rod. The coefficients are scaled by the appropriate factors to yield a numerical evaluation of $D_H(x)$. This is shown as the solid black line in Fig. 4. This shows very good agreement with the analytical approach and justifies the approximation of a uniform surface-charge distribution over the hemispherical endcap.

### B. Coupling to the nanodisk

To investigate the coupling of a molecule to a linearly varying surface-dipole distribution, we consider the nanodisk of Fig. 3 which shows a surface distribution that varies approximately in a linear fashion. We assume that the charge varies in the $\hat{x}_1$ direction so that $\theta=0$ in Eqs. (38) and (39). As before we have a product of eigenfunctions but these now depend on distance with a form $(\tau_p^1 r\cos\phi)(\sigma_p^1 r\cos\phi)$. Since the product of the eigenfunctions integrated over the nanoparticle must give unity, Eq. (1), we set $R_D$ as the radius of interaction of the dipole with the disk and assume that this represents a fraction $f_D$ of the total integral over the surface. Then we have

$$\int_0^{R_D}\int_0^{2\pi} \tau_p^1\sigma_p^1 r^2\cos\phi r dr d\phi = \tau_p^1\sigma_p^1\pi R_D^4/4 \approx f_D, \quad (42)$$

and the product of the geometry-dependent terms is

$$\frac{\alpha\eta_{pd}\eta_{dp}}{8\pi^2} = (\hat{x}_k\,.\,\hat{x}_1)^2 f_l D_D(x)\left(\frac{R_d}{R_D}\right)^3\left(\frac{\epsilon_d/\epsilon_b-1}{\epsilon_d/\epsilon_b+2}\right), \quad (43)$$

where $x=z_d/R_D$ and

$$D_D(x) = 8x\left(1-\frac{2x^2+1}{2x\sqrt{x^2+1}}\right)\left(\frac{x(2x^2+3)}{2(x^2+1)^{3/2}}-1\right). \quad (44)$$

This function and $x^3D_D(x)$ are shown in Fig. 5. As with the hemisphere, the maximum coupling occurs when the dipole is on the surface of the disk and for large disks the coupling is dominated by the $(R_d/R_D)^3$ term. For the molecule situated at a fixed distance, there is an optimum radius of the disk that occurs for $x\approx 0.67$ for which the coupling is maximum.

As with the nanorod, the coupling to the disk was also evaluated numerically. The disk is represented by a polygon of 36 sides of radius 100 units and width 20 units, as shown in Fig. 3. The surface is tesselated with 3320 triangles, the eigenfunctions are determined and the coefficients for the coupling of the sphere to the fundamental mode of the nanodisk are evaluated as a function of the distance of the sphere above the top of the center of the disk. The coefficients were scaled to yield a numerical evaluation of $D_D(x)$, shown by the solid black line in Fig. 5. There is reasonable agreement with the analytical formula, although it is not as good as for the hemisphere. This may be related to the surface-charge and surface-dipole distributions varying only approximately linearly with distance. In particular the distributions deviate more from a linear variation near the edges of the disk. In this regard we would expect the agreement to be poorer as the test sphere moves further away from the disk surface. This behavior is seen in Fig. 5.

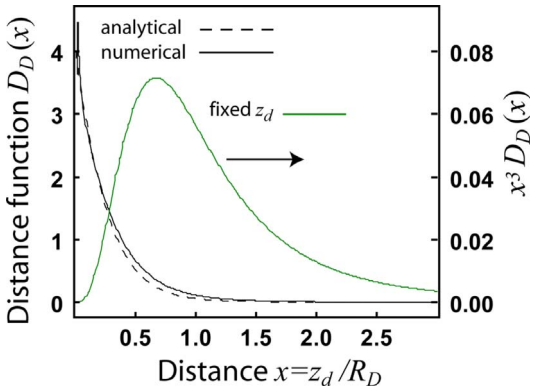


FIG. 5. (Color online) The distance dependent function $D_D(x)$ for the coupling of a molecule to a disk as a function of $x=z_d/R_D$ with the dashed line based on the analytical calculation and the solid black line obtained from a numerical simulation. The function $x^3D_D(x)$ indicates the variation of the coupling with the size of the coupling region for a fixed dipole distance $z_d$.

### C. Sensitivity to the presence of molecules

Finally, we estimate the effect of molecules on both the resonant frequencies and the phase shifts of single nanoparticles using the previously derived results. Apart from the variation of the coupling, which generally is maximum for the molecule on the surface of the nanoparticle, the strength of the interaction depends on the difference between the effective permittivity of the molecule and that of the background medium, which is often a water-based solution. It also depends on the effective size of the molecule, since the polarizability scales with the volume.

We first estimate the wavelength shift based on Eq. (32). From the previous section, a conservative estimate of the coupling of a molecule is $f_H D_H(0)\approx 0.1$. Protein molecules have a typical hydrodynamic radius[35] of $R_d\approx 2$ nm and we assume the radius of the nanorod is $R_H\approx 10$ nm. The expression for the frequency shift involves the eigenvalue of the nanoparticle, which we take as $\gamma_p^1=1.2$. For a protein in a water solution we set $\epsilon_b\approx 1.75$ and for the protein[36] $\epsilon_d \approx 2.25$. Finally we assume that the nanoparticle resonates with incident light of wavelength 800 nm in vacuum and the

nanoparticle is made from a metal with a plasma frequency that is excited by a vacuum wavelength of $\lambda_p \approx 400$ nm. Then using Eqs. (32) and (40) with $\delta\lambda/\lambda_0 = -\delta\omega/\omega_0$ the shift in the wavelength of the resonance of the nanoparticle when the molecule is close to it is $\delta\lambda \approx 0.14$ nm. For comparison, we estimate the phase shift in the resonance of the nanoparticle using Eq. (33) with the same parameters as above. In addition we assume that the imaginary part of the metal permittivity is Im $\epsilon \approx 1$, which is approximately the value for gold at an excitation wavelength of 800 nm. The presence of a molecule then shifts the phase of the resonance by $\Delta\phi \approx 0.5$ degrees.

These estimates depend very strongly on the parameters that describe the nanoparticle and its resonance, as well as on the properties of the molecule. Most important is the geometric coupling, which decreases rapidly with $z_d/R$, and also the ratio of the radius of the molecule and the radius of the surface of interaction, since there is a cubic dependence on this ratio of the shifts in the resonance or the phase. This is a consequence of the volume dependence of the molecule polarizability. A 10% error in the radius will lead to a 30% error in the polarizability and result in a similar error in the estimate of the resonance shift. In practice, however, the actual size of the molecule and its effective permittivity are not measured—rather, the electric properties are obtained from measurements of the molecule polarizability. In comparing Eq. (32) for the frequency shift with Eq. (33) for the phase shift, we see that the frequency shift depends on the eigenvalue $\gamma_p^1$ according to $1/(\gamma_p^{1^2}-1)$ whereas the phase shift depends on the eigenvalue as $1/(\gamma_p^1-1)^2$. For nanorods we have $\gamma_p^1 \approx 1.2$ and the eigenvalue approaches unity as the aspect ratio of the rod becomes larger. This means that the phase shift tends to vary more quickly than the wavelength shift, so that it is more sensitive to variations of the aspect ratio.

The theory that we have developed is based on the electrostatic approximation that does not take account of the reradiation of light from the nanoparticle. While this is important for larger particles, it has been shown that, for nanoparticles much smaller than the wavelength of light, the electrostatic method predicts resonances that compare well with the finite-difference time-domain (FDTD) numerical method.[37] The FDTD method solves Maxwell's equations for the complete electromagnetic field and includes the effects of reradiation. For comparison with the theory that we have developed here, we show in Fig. 6 the resonance shift as a function of $x = z_d/R_H$ calculated using the FDTD method for a dielectric sphere at a fixed height $z_d$ above the nanorod. The solid curve is the calculation based on Eqs. (32) and (40). The parameters used in the model were: $R_d = 5$ nm, $z_d = 5.5$ nm, $\epsilon_d = 2.25$, and $\epsilon_b = 1.75$. The nanorod was made from gold with a cylindrical body 3.75 units long and 1 unit radius with hemispherical endcaps also 1 unit radius. The aspect ratio of the nanorod was kept fixed and the physical dimensions scaled to determine the shift in resonance with the radius $R_H$. It should be noted that there are difficulties in using the FDTD method in this application in that resonances are broad and the shifts are difficult to resolve from the calculated spectra (which is the origin of the error bars in Fig. 6). Furthermore it was not possible to include a point-like dipole in the FDTD model which was replaced by a dielectric sphere. Even so, there is good qualitative agreement between the two methods, with both curves showing an optimum ratio that maximizes the resonance shift and with magnitudes of the resonance shifts similar to our estimates above.

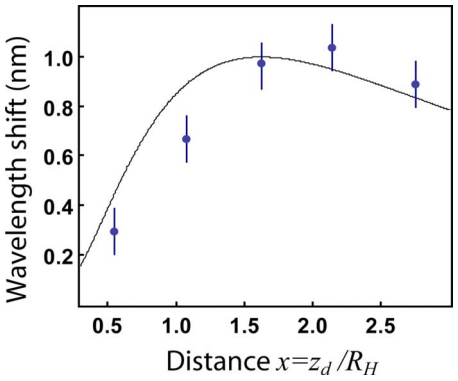


FIG. 6. (Color online) The shift in the wavelength of the resonance of a gold nanorod in the presence of a dielectric sphere as a function of the ratio of sphere height to nanorod radius, calculated using the electrostatic theory (solid curve), and a finite-difference time-domain algorithm (points). The errors relate to the uncertainty in locating the resonance in the calculated spectrum.

## VI. CONCLUSIONS

In this paper we have used an electrostatic coupling theory to model the effects of a molecule on the localized surface plasmon resonances in metallic nanoparticles. The molecule was modeled as a small dielectric sphere and approximate expressions for the coupling coefficients were derived. It was shown that the effect of a molecule near the nanoparticle can be modeled by a change in the local permittivity. For weak coupling, as would be found with small numbers of molecules, the effective permittivity, the frequency shift and the phase shift of the resonance are proportional to polarizability of the molecule and to a geometric factor describing the strength of the interaction and its spatial dependence. By considering simple situations, it was shown that the coupling is maximized when the molecule is resting on the surface of the nanoparticle, which is what we would expect, and that the coupling favors a high radius of curvature. However, in situations where the molecule cannot approach the nanoparticle closer than a fixed distance, there is an optimum dimension of the coupling region on the nanoparticle. It was shown that this is related to the properties of the electric field of the dipole. We considered two simple situations of the coupling of molecules to two nanoparticles, namely, the hemispherical top of a nanorod and to the center of a nanodisk. The results of analytical expressions describing the interactions were compared with more precise numerical calculations, with good agreement.

**ACKNOWLEDGMENTS**

We wish to thank Alison Funston for providing the TEM image of the gold nanorods and Dougal Davis for assistance in evaluating the coupling coefficients.

[1] T. R. Jensen, M. L. Duval, K. L. Kelly, A. A. Lazarides, G. C. Schatz, and R. P. Van Duyne, J. Phys. Chem. B **103**, 9846 (1999).
[2] A. C. Templeton, J. J. Pietron, R. W. Murray, and P. Mulvaney, J. Phys. Chem. B **104**, 564 (2000).
[3] P. Hanarp, M. Kall, and D. Sutherland, J. Phys. Chem. B **107**, 5768 (2003).
[4] J. J. Mock, D. R. Smith, and S. Schultz, Nano Lett. **3**, 485 (2003).
[5] F. Tam, C. Moran, and N. Halas, J. Phys. Chem. B **108**, 17290 (2004).
[6] M. M. Miller and A. A. Lazarides, J. Phys. Chem. B **109**, 21556 (2005).
[7] A. J. Haes, S. L. Zou, G. C. Schatz, and R. P. Van Duyne, J. Phys. Chem. B **108**, 6961 (2004).
[8] G. Raschke, S. Brogi, A. S. Susha, A. L. Rogach, T. A. Klar, J. Feldmann, B. Fieres, N. Petkov, T. Bein, A. Nichtl, and K. Kurzinger, Nano Lett. **4**, 1853 (2004).
[9] S. Lal, S. Link, and N. J. Halas, Nat. Photonics **1**, 641 (2007).
[10] K. A. Willets and R. P. Van Duyne, Annu. Rev. Phys. Chem. **58**, 267 (2007).
[11] A. D. McFarland and R. P. Van Duyne, Nano Lett. **3**, 1057 (2003).
[12] J. N. Anker, W. Paige Hall, O. Lyandres, N. C. Shah, J. Zhao, and R. P. Van Duyne, Nature Mater. **7**, 442 (2008).
[13] M. Duval Malinsky, K. L. Kelly, G. C. Schatz, and R. P. Van Duyne, J. Phys. Chem. B **105**, 2343 (2001).
[14] M. W. Knight, Y. Wu, J. B. Lassiter, P. Nordlander, and N. J. Halas, Nano Lett. **9**, 2188 (2009).
[15] T. J. Davis, K. C. Vernon, and D. E. Gómez, J. Appl. Phys. **106**, 043502 (2009).
[16] T. J. Davis, K. C. Vernon, and D. E. Gómez, Phys. Rev. B **79**, 155423 (2009).
[17] I. D. Mayergoyz, D. R. Fredkin, and Z. Zhang, Phys. Rev. B **72**, 155412 (2005).
[18] P. Grossel, D. Van Labeke, and J.-M. Vigoureux, Chem. Phys. Lett. **99**, 193 (1983).
[19] I. A. Larkin, M. I. Stockman, M. Achermann, and V. I. Klimov, Phys. Rev. B **69**, 121403(R) (2004).
[20] P. G. Etchegoin and E. C. Le Ru, J. Phys.: Condens. Matter **18**, 1175 (2006).
[21] P. Anger, P. Bharadwaj, and L. Novotny, Phys. Rev. Lett. **96**, 113002 (2006).
[22] S. Gerber, F. Reil, U. Hohenester, T. Schlagenhaufen, J. R. Krenn, and A. Leitner, Phys. Rev. B **75**, 073404 (2007).
[23] A. Trügler and U. Hohenester, Phys. Rev. B **77**, 115403 (2008).
[24] J.-Y. Yan, W. Zhang, S. Duan, X.-G. Zhao, and A. O. Govorov, Phys. Rev. B **77**, 165301 (2008).
[25] U. Hohenester and A. Trügler, IEEE J. Sel. Top. Quantum Electron. **14**, 1430 (2008).
[26] M. S. Tomas and Z. Lenac, Opt. Commun. **100**, 259 (1993).
[27] G. W. Ford and W. H. Weber, Phys. Rep. **113**, 195 (1984).
[28] I. D. Mayergoyz, Z. Zhang, and G. Miano, Phys. Rev. Lett. **98**, 147401 (2007).
[29] T. J. Davis, K. C. Vernon, and D. E. Gómez, Proc. SPIE **7394**, 739423 (2009).
[30] D. J. Bergman, Phys. Rev. B **19**, 2359 (1979).
[31] D. J. Bergman and D. Stroud, Phys. Rev. B **22**, 3527 (1980).
[32] J. D. Jackson, *Classical Electrodynamics* 2nd ed (Wiley, New York, 1975).
[33] C. F. Bohren and D. R. Huffman, *Absorption and Scattering of Light by Small Particles* (Wiley, New York, 1973).
[34] A. M. Funston, C. Novo, T. J. Davis, and P. Mulvaney, Nano Lett. **9**, 1651 (2009).
[35] O. Tcherkasskaya, E. A. Davidson, and V. N. Uversky, J. Proteome Res. **2**, 37 (2003).
[36] S. Johnsen and E. A. Widder, J. Theor. Biol. **199**, 181 (1999).
[37] T. J. Davis, K. C. Vernon, and D. E. Gómez, Opt. Express **17**, 23655 (2009).